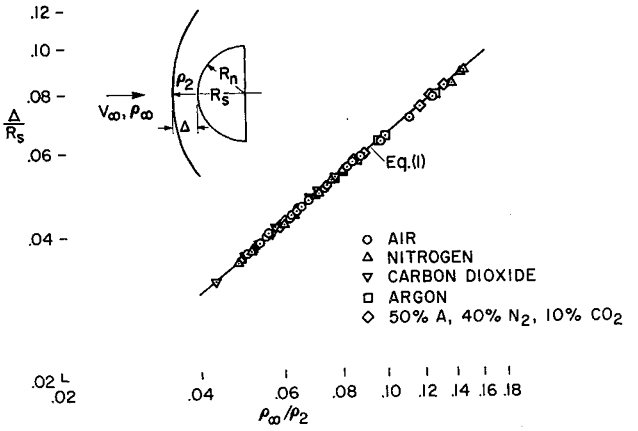

a)

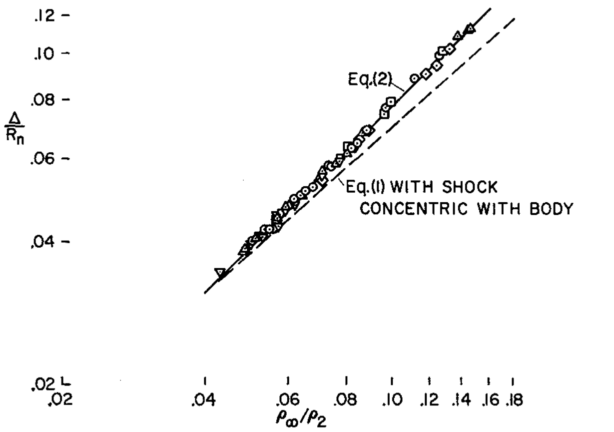

b)

Fig. 1 Shock standoff distance as a function of density ratio across normal shock: a) Δ/R_s and b) Δ/R_n.

density ratio across a normal shock. In Fig. 1a the standoff distance Δ is normalized by R_s, the radius of curvature of the shock at the axis of symmetry. In this form the numerical results are correlated by the constant-density solution of Hayes and Probstein[3]:

$$\frac{\Delta}{R_s} = \frac{\rho_\infty/\rho_2}{1 + (8\rho_\infty/3\rho_2)^{1/2}} \tag{1}$$

Of more interest to the designer is the shock standoff distance normalized by R_n, the nose radius (Fig. 1b). The constant-density analysis by Hayes and Probstein does not yield the nose radius; hence, it is necessary to make a further

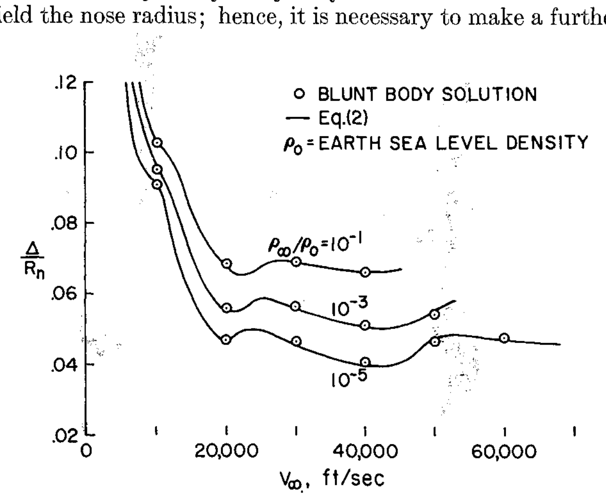

Fig. 2 Shock standoff distance for mixture of 50% argon, 40% nitrogen, and 10% carbon dioxide; T_∞ = 634° R.

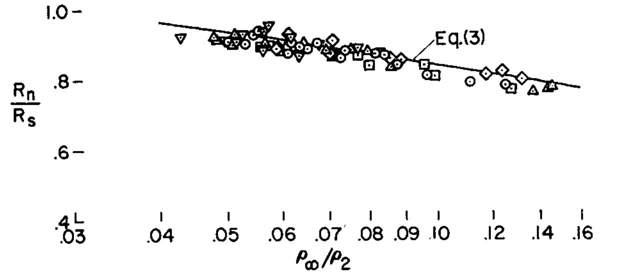

Fig. 3 Ratio of nose radius to shock radius.

assumption, for example, that the shock and body are concentric, in order to relate the standoff distance to the nose radius. This assumption is not valid as shown in Fig. 1b. However, the present numerical results are correlated by a simple linear law found by Seiff[4]:

$$\Delta/R_n = 0.78(\rho_\infty/\rho_2) \tag{2}$$

A typical variation of standoff distance with freestream velocity and density is shown in Fig. 2 for the mixture of argon, nitrogen, and carbon dioxide.

The ratio of nose radius to shock radius from the present numerical method is shown in Fig. 3. Combination of Eqs. (1) and (2) yields the following correlation equation:

$$\frac{R_n}{R_s} = \frac{1.28}{1 + (8\rho_\infty/3\rho_2)^{1/2}} \tag{3}$$

References

[1] Lomax, H. and Inouye, M., "Numerical analysis of flow properties about blunt bodies moving at supersonic speed in an equilibrium gas," NASA TR R-204 (1964).

[2] Klaimon, J. H., "Hypersonic flow field around a hemisphere in a CO_2-N_2-A gas mixture," AIAA J. **2**, 953–954 (1964).

[3] Hayes, W. D. and Probstein, R. F., *Hypersonic Flow Theory* (Academic Press Inc., New York, 1959), pp. 158–162.

[4] Seiff, A., "Recent information on hypersonic flow fields," *Gasdynamics in Space Exploration*, NASA SP-24 (1962).

Heat Transfer from an Impinging Rocket Jet

D. A. Cose* and B. T. Lee*

United Technology Center, Sunnyvale, Calif.

Nomenclature

A = area, ft^2
C_p = specific heat, Btu/lb-°F
h = heat-transfer coefficient, Btu/ft^2-°F-sec
k = thermal conductivity, Btu/ft-sec-°F
l = length into plate, ft
Pr = Prandtl number
q = heat flow rate, Btu/sec
t = time, sec
M = average molecular weight
T = temperature, °F
U = velocity, fps
W = weight, lb
X = distance from start of boundary layer, ft
γ = specific heat ratio
ρ = density, lb/ft^3
μ = viscosity, lb/in.-sec

Subscripts

g = gas
0 = stagnation
P = plate
R = reference

Received August 7, 1964.

* Aerothermo Engineer, Engineering Sciences Branch.

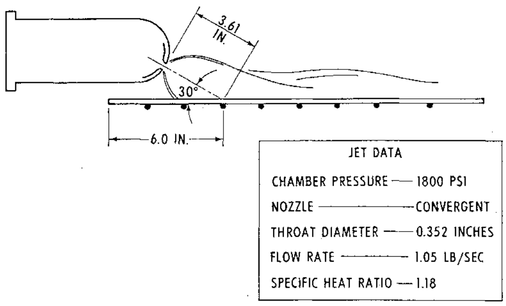

Fig. 1 Experimental arrangement.

DETERMINATION of heat transfer from supersonic rocket jets impinging on adjacent surfaces is important in rocket technology. The exhaust jet will generally impinge on portions of the launch platform and tower during liftoff, or staging rocket jets will possibly impinge on the vehicle upper stages during separation and may cause mission failure. These heat-transfer problems become more important as booster sizes increase and missions and launch facilities become more complex.

A corollary problem exists through the use of pyrotechnics to ignite solid-propellant rocket motors. As solid booster sizes are increased, the possibility of significant weight savings through accurate igniter sizing is also increased. However, to optimize igniter size, it is necessary that ignition pressure transients, which are strong functions of propellant surface heat transfer, be calculable.

Heat transfer from subsonic jet impingement has been studied,[1–3] and some supersonic jet impingement data exist,[4–6] but experimental data concerning impingement heat transfer from supersonic, solid rocket jets containing alumina particles are not available. The calculation of impingement heat transfer is complicated by the two-phase nature of the jet, radiation from the jet, afterburning on the jet surface, and the energy transfer caused by solid particles solidifying on the surface. Each of these complexities make an analytical study of impingement heating extremely difficulty, if not impossible.

Flow in a supersonic jet impinging on a solid surface will go through a normal shock or a series of oblique shocks to establish some flow regime downstream of the impingement zone. One method that should provide a fairly accurate estimate of the convective component of heat transfer outside the impingement region would be to assume turbulent flat-plate flow with the boundary layer starting at the impingement zone. A turbulent boundary layer, by its very nature, responds rapidly to varying wall temperature, and consequently it is not a strong function of its history to a particular point on the wall. This convenient phenomenon allows one to calculate heat-transfer rates without regard to upstream wall temperature variations. However, as calculations approach the impingement zone or the starting point of the boundary layer, turbulent flat-plate theory breaks down and heat-transfer rates approach infinity. To gain additional information about where turbulent flat-plate theory would be applicable, an experimental program was initiated to measure heat transfer in the impingement region.

The experimental apparatus consisted of a two-phase, solid rocket jet expanding through a sonic nozzle from a chamber pressure of 1800 psi and impinging on a thin (0.129-in.-thick) copper plate (Fig. 1). The plate was divided into two sections: one highly polished to minimize radiative heat transfer, and the other sprayed with a thin coating of flat black paint to maximize radiative heat transfer. The objective of the painting was to provide a method to separate the radiative and convective heat transfer. The plate temperature was monitored during the test at 25 locations by 30-gage chromel-constantan thermocouples attached to the back side of the plate approximately 0.10 in. from the hot gas surface.

The relative thinness of the plate permits the assumption that heat flow will be one-dimensional. Also, the temperature-time response of a thermocouple located on the back side of a 0.10-in.-thick copper plate was analytically determined to insure that valid heat-transfer data could be measured and that the hot-side surface would not melt during the $\frac{1}{2}$-sec test duration. The plate response for a typical expected heat-transfer coefficient is presented in Fig. 2, which indicates that valid data can be obtained after 15 msec. After 15 msec, the expression for the heat flux can be written

$$\dot{q} = hA(T_{og} - T_p) = WC_p(dT_p/dt) \tag{1}$$

which can be approximated in finite difference form as

$$\frac{\Delta T_p}{\Delta t} = \frac{h(T_{og} - T_p)}{\rho C_p l} \tag{2}$$

The convective heat-transfer coefficient for fully turbulent flow over a flat plate is given by

$$h(P_R)^{2/3}/C_p\rho_R U = 0.0296(\mu/\rho_R UX)^{0.2} \tag{3}$$

Test Results

The impingement zone boundaries were well defined experimentally by the deposition of aluminum oxide on the

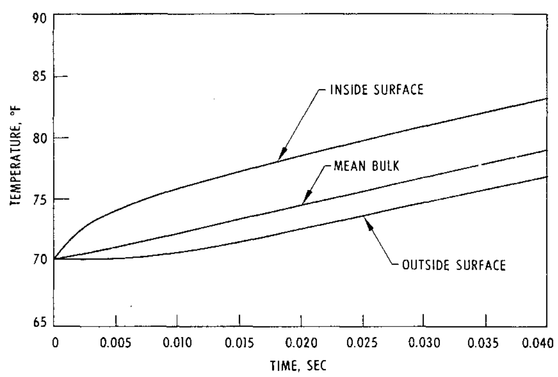

Fig. 2 Temperature-time responses of a copper plate.

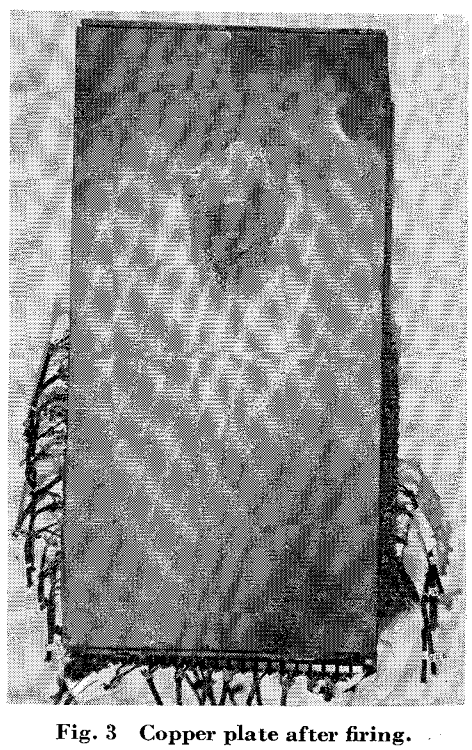

Fig. 3 Copper plate after firing.

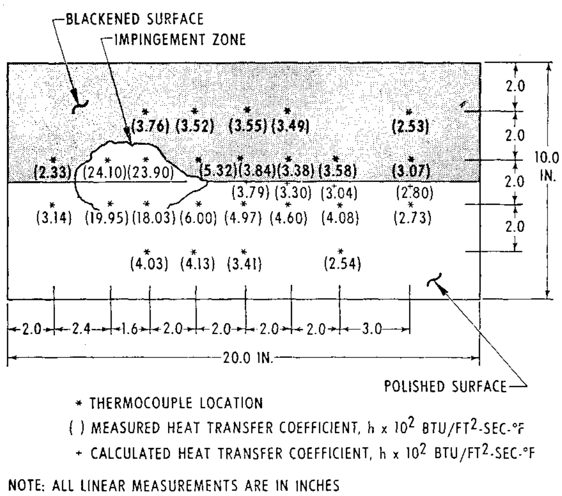

Fig. 4 Map of heat-transfer coefficients.

copper plate. Also evident were general flow lines and patterns (see Fig. 3). As would be expected, the area directly in line with the nozzle received severe deposition, but areas to the side and downstream received much less. The areas upstream of impingement received slight or no deposition. A map of the calculated and measured heat-transfer coefficients is presented in Fig. 4.

Turbulent flat-plate heat-transfer coefficients were estimated using Eq. (3) and the following expressions and assumptions to calculate gas properties:

$$C_p = \gamma R/(\gamma - 1)$$

$$P_R = 4\gamma/(9\gamma - 5)$$

$$\mu_R = 46.6 \times 10^{-10}(M)^{1/2}(T)_R{}^6 \text{ lb/in.-sec} \qquad (3a)$$

The quantity ρu was approximated from the average mass flow from the igniter and the jet cross-sectional area immediately before impingement. The quantity $(T_{og} - T_p)$ for the experimental conditions was taken to be approximately 5000°F. As can be seen, the experimental values are slightly higher than the analytical, which may be due to aluminum oxide solidifying on the surface, or possibly the quantity $(T_{og} - T_p)$ is less than the approximated 5000°F. However, the turbulent flat-plate theory does predict the correct level of the heat-transfer coefficient.

The effects of radiation were most visible in the impingement zone. In this region, radiation was approximately 20% of the total heat transfer; outside this area, the contribution was indiscernible. At some locations, the thermocouples behind the painted surface indicated lower over-all heat transfer than those behind the polished surface, possibly because of the insulating effect of the paint.

Heat transfer in the impingement zone was 500 to 600% higher than a turbulent boundary-layer analysis would predict; this was much higher than the single-phase data of Ref. 6, which indicated an increase of 20%. Therefore, the two-phase nature of the jet (i.e., the alumina particles) probably are responsible for the large increase in heat transfer.

After firing, the deposited aluminum oxide was scraped from the direct impingement zone and weighed. The weight deposited divided by the deposition area and the firing duration gave a deposition rate equal to approximately 1.5% of the total particle flow rate.

Conclusions

Stagnation heat transfer, solidification of alumina particles, and radiation were the important modes of heat transfer in the impingement zone. Outside the impingement area, radiation and solidification were relatively unimportant; therefore, the greatest heat transferred was from convection, and turbulent boundary-layer theory is applicable. Although the actual heat transferred in a short flow region following the impingement zone was higher than indicated by turbulent boundary-layer theory, the theory can provide a fair estimate of the actual heat transferred.

References

[1] Shirnow, V. A., Verevochkin, E. E., and Brdlick, P. H., "Heat transfer between a jet and a held plate normal to flow," Intern. J. Heat Mass Transfer, 2 1–7 (1961).

[2] Myers, G. E., Schauer, J. J., and Eustis, R. H., "The plane turbulent wall jet," Parts 1 and 2, Dept. of Mechanical Engineering, Stanford Univ. TR 1 and 2, National Science Foundation Grant G9705 (1961).

[3] Metzer, D. E., "Spot cooling and heating of surfaces with impinging air jets," Dept. of Mechanical Engineering, Stanford Univ. TR 52, Contract NONR 225(23) (April 1962).

[4] Bauer, R. C. and Schlumpf, R. L., "Experimental investigation of free jet impingement on a flat plate," Arnold Engineering Development Center, AEDC TN 60-223 (March 1961).

[5] Stitt, L. E., "Interaction of highly underexpanded jets with simulated lunar surfaces," NASA TN-D-1095 (December 1961).

[6] Huang, G. C., "Investigations of heat transfer coefficients for air flow through round jets impinging normal to a heat transfer surface," American Society of Mechanical Engineers, Paper 62-HT-31 (1962).

Buckling of Axially Compressed Cylindrical Shells Reinforced by Circumferential Fiber Windings

H. L. LANGHAAR* AND A. P. BORESI*
University of Illinois, Urbana, Ill.

AND

G. LOVE† AND L. MARCUS‡
General Motors Corporation, Indianapolis, Ind.

1. Introduction

METAL cylinders designed to withstand internal pressure are sometimes prestressed by circumferential filament windings, so that the axial and circumferential stresses in the cylinders are approximately equalized when the internal pressure acts. The lateral deflections and the initial stresses caused by the windings may conceivably reduce the capacity of such a cylinder to withstand an axial compressive force. Apparently, the windings have little effect on the elastic stability if they are bonded to the cylinder, since they cannot affect the net tractions N_x, N_θ, $N_{x\theta}$ in the composite structure. However, the situation is different if the fibers are free to slip on the cylinder when buckling occurs. This case is investigated for isotropic elastic cylinders in the present analysis. The infinitesimal theory of buckling is used. It is known that this theory gives axial buckling loads of cylinders higher than those observed in tests. Nevertheless, the infinitesimal theory yields an indication of the relative importance of the windings on the stability of the shell.

We suppose that there are no end constraints when the windings are applied. The effect of the windings is to cause a constant radial deflection w_0. After the shell is wound, end plates are inserted, and the shell is subjected to axial com-

Received January 29, 1964; revision received October 5, 1964. This investigation was performed for the Allison Division of General Motors Corporation, at the request of H. E. Helms. The results of Table 1 were computed by Allison.

* Professor of Theoretical and Applied Mechanics.
† Stress Analyst, Allison Division.
‡ Numerical Analysts, Allison Division.